

Data quality monitors of vertex detectors at the start of the Belle II experiment

Peter Kodyš^{1,}, Jesus Abudinen², Karlheinz Georg Ackermann³, Karol Mateusz Adamczyk⁴, Patrick Ahlburg⁵, Hiroaki Aihara⁶, Oscar Alonso⁷, Mohammed Albalawi⁸, Ladislav Andricek⁹, Rachid Ayad⁸, Tariq Aziz¹⁰, Varghese Babu¹¹, Szymon Grzegorz Bacher⁴, Seema Bahinipati¹², Giovanni Batignani¹³, Jerome Baudot¹⁴, Prafulla Kumar Behera¹⁵, Stefano Bettarini¹³, Tadeáš Bilka¹, Marca Boronat¹⁶, Andrzej Bozek⁴, Nils Braun¹⁷, Florian Buchsteiner¹⁸, Allen Caldwell³, Christian Camien¹¹, Giulia Casarosa¹³, Daniel Cervenkov¹, Vladimir Chekelian³, Yeqi Chen¹⁹, Luigi Corona¹³, Thomas Rafael Czank²⁰, Sanjeeda Bharati Das²¹, Nibedita Dash¹⁵, Gaetano de Marino¹³, Bruno Deschamps⁵, Angel Dieguez⁷, Jochen Dingfelder⁵, Zdeněk Doležal¹, Giulio Dujany¹⁴, Daniel Esperante¹⁶, Francesco Forti¹³, Markus Fras³, Ariane Frey²², Markus Friedl¹⁸, Juan Fuster¹⁶, Miroslav Gabriel³, Karsten Gadow¹¹, Eldar Ganiev², Uwe Gebauer²², Thomas Gessler²³, Georgios Giakoustidis⁵, Luigi Li Gioi³, Benigno Gobbo², Pablo Gomis López¹⁶, Daniel Greenwald²⁴, Yinghui Guan²⁵, Soumen Halder¹⁰, Koji Hara²⁶, Oskar Hartbrich²⁷, Sagar Hazra¹⁰, Martin Heck¹⁷, Tomasz Hemperek⁵, Martin Hensel⁹, Takeo Higuchi²⁰, Matthias Hoek²⁸, Stefan Huber²⁴, Ryosuke Itoh²⁶, Christian Irmeler¹⁸, Akimasa Ishikawa²⁶, Hyebin Jeon²⁹, Changwoo Joo²⁰, Mateusz Kaleta⁴, Abdul Basith Kaliyar¹⁰, Jakub Kandra¹, Kookhyun Kang²⁹, Piotr Julian Kapusta⁴, Christian Kiesling³, Bartłomiej Kisielewski⁴, David Kittlinger³, Daniel Klose⁹, Christian Koffmane⁹, T. Kohriky²⁶, Tomoyuki Kono³⁰, Igor Konorov²⁴, Silvia Krivokuca⁹, Hans Krüger⁵, Thomas Kuhr³¹, Manish Kumar²¹, Rajeev Kumar³², Peter Kvasnička¹, Carlos Lacasta¹⁶, Chiara La Licata²⁰, Kavita Lalwani²¹, Livio Lanceri², Jens Sören Lange²³, Klemens Lautenbach²³, Seungcheol Lee²⁹, Ulrich Leis³, Philipp Leitl³, Dmytro Levit²⁴, Chunhua Li³³, Y. B. Li³⁴, James Frederick Libby¹⁵, Gerhard Liemann⁹, Qingyuan Liu³⁵, Zhen'An Liu³⁶, Thomas Lück^{13,31}, Florian Luetticke⁵, Lydia Macharski¹¹, Souvik Maity¹², Carlos Mariñas¹⁶, Sukant Narendra Mayekar¹⁰, Sara Mccarney³, Gagan Bihari Mohanty¹⁰, Johnny Alejandro Mora Grimaldo⁶, Tomoko Morii²⁰, Hans-Günther Moser³, David Moya³⁷, Felix Johannes Müller¹¹, Felix Müller³, Katsuro Nakamura²⁶, Mikihiro Nakao²⁶, Zbigniew Marian Natkaniec⁴, Carsten Niebuhr¹¹, Jelena Ninkovic⁹, Yoshiyuki Onuki⁶, Waclaw Ostrowicz⁴, Antonio Paladino¹³, Eugenio Paoloni¹³, Hwanbae Park²⁹, SeokHee Park³⁸, Botho Paschen⁵, Stephan Martin Paul²⁴, Ivan Peric¹⁷, Frauke Poblitzki¹¹, Andrei Rabusov²⁴, K. K. Rao¹⁰, Simon Reiter²³, Rainer Helmut Richter⁹, Isabelle Ripp-Baudot¹⁴, Martin Ritter³¹, Michael Ritzert³⁹, Giuliana Rizzo¹³, Niharika Rout¹⁵, Debashis Sahoo¹⁰, Javier Gonzalez Sanchez³⁷, Luka Santelj⁴⁰, Nobuhiko Sato²⁶, Bianca Scavino²⁸, Gerhard Schaller⁹, Martina Schnecke⁹, Florian Schopper⁹, Harrison Schreeck²², Christoph Schwanda¹⁸, Benjamin Schwenker²², Reinhard Sedlmeyer⁹, Concettina Sfienti²⁸, Frank Simon³, Sebastian Skambraks⁹, Yuri Soloviev¹¹, Björn Spruck²⁸, Slavomira Stefková¹¹, Reimer Stever¹¹, Ulf Stolzenberg²², Soh Yamagata Suzuki²⁶, Maiko Takahashi¹¹, Eva Tafelmayer⁹, Shuji Tanaka²⁶, Hikaru Tanigawa⁶, Richard Thalmeier¹⁸, Toru Tsuboyama²⁶, Yuma Uematsu⁶, O. Verbycka⁴, Ivan Vila³⁷, Amparo Lopez Virto³⁷,*

*e-mail: peter.kodyš@mff.cuni.cz

Lorenzo Vitale², Sven Vogt³, Marcel Vos¹⁶, Kun Wan⁶, Boqun Wang³, Shun Watanuki⁴¹, James Webb⁴², Norbert Wermes⁵, Christian Wessel⁵, Jarosław Paweł Wiechczyński¹³, Philipp Wieduwilt²², Hendrik Windel⁹, Satoru Yamada²⁶, Hua Ye¹¹, Hao Yin¹⁸, Laura Zani¹³, and Tingyu Zhang⁶ for the Belle II PXD, SVD, DAQ, DQM and software collaborations

¹Charles Univ. Prague, Czech Republic

²INFN and Univ. Trieste, Italy

³Max Planck Institut für Physik Muenchen, Germany

⁴Institute of Nuclear Physics PAN, Poland

⁵Univ. of Bonn, Germany

⁶U-Tokyo, Japan

⁷University of Barcelona, Spain

⁸Univ. of Tabuk, Saudi Arabia

⁹Semiconductor Laboratory of the Max Planck Society, Germany

¹⁰Tata Institute of Fundamental Research, India

¹¹Deutsches Elektronen-Synchrotron(DESY), Germany

¹²Indian Institute of Technology Bhubaneswar, India

¹³INFN and Univ. Pisa, Italy

¹⁴Institut Pluridisciplinaire Hubert Curien (IPHC) Strasbourg, France

¹⁵Indian Institute of Technology Madras, India

¹⁶Instituto de Fisica Corpuscular(IFIC), Spain

¹⁷Karlsruhe Institute of Technology(KIT), Germany

¹⁸Institute of High Energy Physics, Austrian Academy of Sciences, Austria

¹⁹Univ. of Science and Technology of China(USTC), China

²⁰Kavli IPMU (WPI), the University of Tokyo, Japan

²¹Malaviya National Institute of Technology Jaipur, India

²²Univ. of Goettingen, Germany

²³Univ. of Giessen, Germany

²⁴Technical Univ. of Munich(Technische Universitaet Muenchen), Germany

²⁵University of Cincinnati, U.S.A.

²⁶High Energy Accelerator Research Organization (KEK), Japan

²⁷Univ. of Hawaii, U.S.A.

²⁸Johannes Gutenberg Univ. of Mainz, Germany

²⁹Kyungpook National Univ.(KNU), South Korea

³⁰Kitasato University, Japan

³¹Ludwig Maximilians Univ. Muenchen(LMU), Germany

³²Panjab Univ., India

³³LiaoNing Normal University(LNNU), China

³⁴Peking Univ.(PKU), China

³⁵Fudan Univ., China

³⁶Institute of High Energy Physics(IHEP), China

³⁷Instituto de Fisica de Cantabria, Spain

³⁸Yonsei Univ., South Korea

³⁹Heidelberg University, Germany

⁴⁰Univ. of Ljubljana, Slovenia

⁴¹Laboratoire de L'accelerateur Lineaire (LAL) Orsay, France

⁴²Univ. of Melbourne, Australia

Abstract. The Belle II experiment features a substantial upgrade of the Belle detector and will operate at the SuperKEKB energy-asymmetric e^+e^- collider at KEK in Tsukuba, Japan. The accelerator completed its first phase of commissioning in 2016, and the Belle II detector saw its first electron-positron collisions in April 2018. Belle II features a newly designed silicon vertex detector based on double-sided strip layers and DEPFET pixel layers. A subset of

the vertex detector was operated in 2018 to determine background conditions (Phase 2 operation). The collaboration completed full detector installation in January 2019, and the experiment started full data taking.

This paper will report on the final arrangement of the silicon vertex detector part of Belle II with a focus on online monitoring of detector conditions and data quality, on the design and use of diagnostic and reference plots, and on integration with the software framework of Belle II. Data quality monitoring plots will be discussed with a focus on simulation and acquired cosmic and collision data.

1 Introduction

The Belle II experiment uses the asymmetric (4 GeV e^+ , 7 GeV e^-) SuperKEKB collider at the High Energy Accelerator Research Organization (KEK) in Tsukuba, Japan. The design peak luminosity is $8 \times 10^{35} \text{ cm}^{-2}\text{s}^{-1}$, about 40 times larger than in the previous Belle experiment, aiming at an integrated luminosity of 50 ab^{-1} [2].

The requirements on the new Belle II vertex detector were high: it had to achieve excellent vertexing and tracking capabilities at higher event rates, beam backgrounds, considerable noise occupancy, and radiation damage.

The vertex detector, VXD (Fig. 1), is one of the critical determinants of the Belle II physics performance. The six-layer detector contains four outer layers of 300 - 320 μm thick double-sided strip sensors (SVD); the two innermost layers are 75 μm thick depleted p-channel FET (DEPFET) sensors (PXD). The full installation of the vertex detector was completed in January 2019, and the detector took its first physics collision data in March 2019.

2 The Silicon Vertex Detector of Belle II

The strip layers of the Belle II VXD use double-sided silicon microstrip sensors read out by APV25 front-end chips, initially developed for the readout system of the CMS experiment at CERN [1]. With 50 ns shaping time and six or three samples per hit, SVD allows precise hit timing at the level of nanoseconds, efficient noise reduction, and separation of signal from background. The sensors have 768 strips on the p-side, and 512 (768 in layer 3) strips on the n-side. A charge injection feature provides strip-by-strip charge response calibration. The SVD comprises 172 detectors arranged in 4 layers with radii 39 mm, 80 mm, 104 mm, and 135 mm, with a total length of 600 mm and a total sensor area of $\sim 1.2 \text{ m}^2$ [2].

The design of Belle II VXD foresaw two DEPFET pixel layers. The DEPFET structure [2] provides in-pixel amplification of detector signals to equivalent current. Layer radii are 14 and 22 mm, and the length is 120 mm. All 14 ladders of Layer 1 were installed, but, due to a series of assembly accidents, only two ladders of Layer 2 were installed to make up for a faulty underlying sensor in Layer 1.

3 VXD data quality monitoring

The main components and flow of data in the VXD data acquisition system are shown schematically in Fig. 2. Event builder 1 collects detector data from all subdetectors except the PXD and sends them for processing to the High-Level Trigger (HLT) cluster, which does fast reconstruction to identify interesting events. The HLT produces some data quality monitoring



Figure 1. A half-shell of the vertex detector during installation. All VXD layers are exposed.

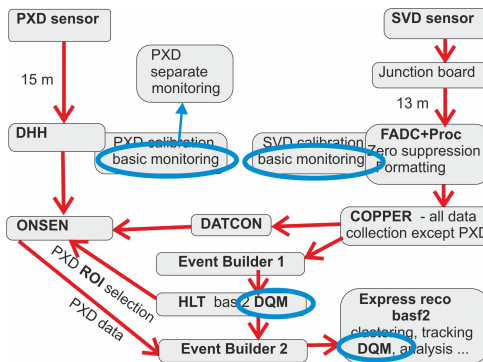


Figure 2. Data flow (red arrows) for the Belle II vertex subdetectors. The blue markings show data quality monitoring modules.

(DQM) data that are then sent to the DQM server. Event Builder 2 adds PXD data to the data of other detectors and sends a subset to the ExpressReco cluster for express reconstruction (up to vertexing). The primary purpose of express reconstruction is online data quality monitoring to check that detectors, slow- and run control work correctly and produce useful data - it produces other DQM data and sends them to the DQM server. The overall bandwidth of the data quality monitoring stream is up to 20-30 MB/s.

Pixels (Fig. 2) are read and signals are processed with the Drain Current Digitizer (DCD) and Data Handling Processor (DHP) chips mounted on the sensor ladder. These chips prepare data for the first compression step using pedestal suppression and for transfer to the Data handling Hub (DHH) [3].

An important side-task of the HLTs is fast online track finding and selection of regions-of-interest (ROIs) on PXD sensors based on track projections from the SVD. This mechanism reduces the amount of raw data produced by the PXD by an order of magnitude.

DHH sends data to the Belle II data chain over Online Selection Nodes (ONSEN) [4]. Via an independent network, data are also sent to a separate system for local calibration of PXD sensors and low-level data quality control. ONSEN combines data for export to Event Builder 2. It can buffer up to 2.5 seconds of data flow and reduce the raw data volume by a factor of 30.

Strip detector signals are transferred over Junction Boards to Flash Analog-to-Digital Converter modules (FADC) for zero suppression and data formatting. Local SVD data quality monitoring and calibration generators use data from this phase of data processing. The signal

is then processed on the COMmon Pipelined Platform for Electronics Readout (COPPER [5]) boards of the central Belle II DAQ for the HLT and Event Builder 1. Apart from that, data are also sent to the PXD ROI finding and data reduction blocks. PXD ROIs are built using both the HLT and the data concentrator (DATCON) modules that find track candidates and then ONSEN extracts PXD data from the ROIs. [4].

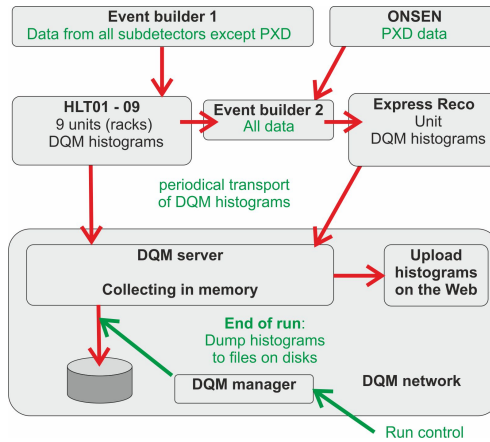


Figure 3. Data workflow for quality monitor of the PXD and SVD subdetectors. Red arrows represent data flows, green markings represent DQM.

4 DQM data production

Data monitors provide a condensed overview of the essential aspects of detector performance. They allow fast discovery of detector problems and identification of their sources so that we can prevent significant data losses and achieve uniformly high data quality. More than 7500 histograms are updated every 2 minutes. Separate sets of DQM histograms are produced by HLT and by Express Reco, cf. Fig. 2.

At Belle II, ExpressReco runs full basf2 [6] reconstruction (up to vertexing) on a sampled data flow from all subdetectors, including the PXD. The sampling rate is adjusted based on the immediate trigger rate. Histogram production for data quality monitoring is the primary purpose of ExpressReco. These and HLT DQM histograms are collected by the DQM server and uploaded to the Web for Control Room or remote presentation. Also, at the end of each run, histograms are saved to disk. DQM Control computer manages DQM data processing and communicates with the Run Control system.

ExpressReco monitors confirm data quality and identify runs usable for further processing. They provide a finer footprint of the data allowing to reveal any irregularities in the data acquisition chain and detector settings.

The collection of data for DQM uses the basf2 framework [6] running on a set of isolated computers (HLT and ExpressReco) with conservative update plans to ensure the stability of production-critical processing. Any outside connections to databases or public networks are forbidden; only local services are allowed.

5 Scope of DQM monitoring

The VXD data quality monitoring system provides several hundred plots of various quantities. Part of them is intended for expert shifters to diagnose sources of DAQ problems. Automatic comparisons with reference data are provided together with color-coded plot canvases indicating serious deviations from reference (green plot frame meaning no problem) so that problems can be spotted quickly among a large number of plots.

A more restricted set of plots is selected for monitoring by Control Room (CR) shifters so that they can spot problems quickly, even without expert knowledge about individual sub-detectors. In case of problems or unclear situations, the CR shifter can inform expert detector shifters by a dedicated chat channel, e-mail, or phone. Any problems are logged, and shifters can subsequently label runs as OK or problematic.

Shifters can also consult run-by-run comparisons of selected sets of variables. Fig. 4 shows the PXD efficiency over runs taken between 15 November and 12 December 2019; a hovering window shows details for the run at the mouse cursor (in this case, run 5695). Fig. 5 shows a similar plot for the SVD, efficiency in u and v strips.



Figure 4. Run-by-run comparison for PXD efficiency. Highlighted run 5695, 8 December 2019.

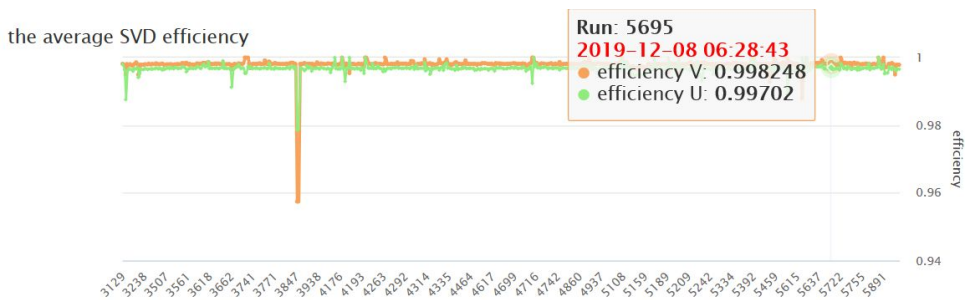


Figure 5. Run-by-run comparison for SVD efficiency in u and v strips. Highlighted run 5695, 8 December 2019.

Basic sensor-by-sensor plots available for Control Room shifters are shown in Figs. 6 (PXD) and 7 (SVD). Reference profiles are available for some plots. Errors or out-of-range conditions are signaled by green-to-red transition(s) of the respective plot frame(s). Data in these plots are from Run 5695, 8 December 2019.

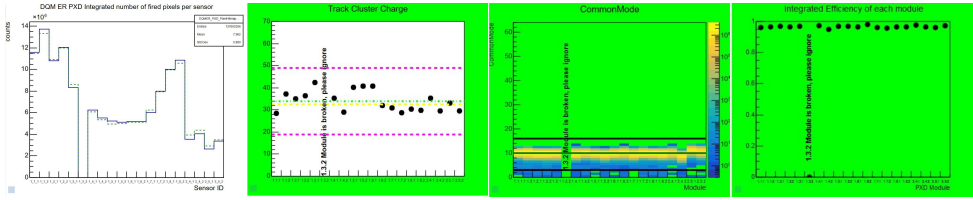


Figure 6. Basic PXD diagnostic plots available for Control Room shifters, left to right: Fired pixels per sensor for each sensor; Cluster charge MPV; Common mode correction in U direction (in rows); Sensor efficiency.

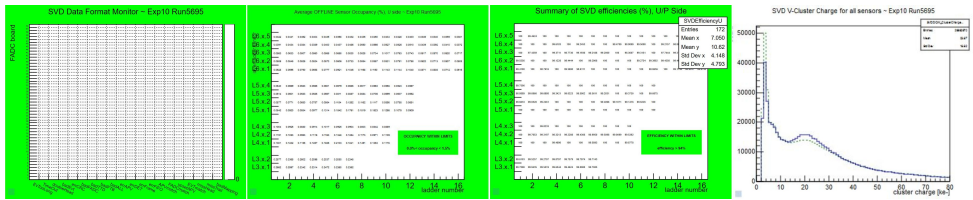


Figure 7. Basic SVD diagnostic plots available for Control Room shifters, left to right: Chip monitor (APV25-to-FADC-to-sensor mapping and status); Occupancy in U strips; Efficiency; Cluster charge in V direction.

6 Optimizing the DQM: cleaner plots, refresh rates and reference plots

For production monitoring, we aim at plots requiring minimum visual processing by the shifter. Where available, plots also display reference data. The software automatically compares actual data with the reference, and canvas color is changed if a mismatch is found. Special efforts go into the development of DQM modes, such as cosmic acquisition, machine adjustment, detector tuning, or beam collisions with different conditions. For this, the DQM will get a database interface to allow straightforward and automated re-configuration. The PXD and SVD groups invest considerable effort into understanding machine background radiation at beam conditions. These efforts can only partially rely on simulations and require, instead, handy data summaries that are available over long times and different conditions. DQM data seem to provide a useful tool for these observational studies. DQM data serve as data summaries also in the study of detector radiation damage: Slow changes in DQM data can be found in the historical record of DQM data and calibrations; also, the update frequency of reference data are an indication of changes in the detectors. All DQM plots are recorded on a dedicated web site with a refresh rate of ~ 2 minutes. The web site provides access to the full history of all DQM plots by run and category, and also allows access to underlying raw datasets.

7 Conclusions

Belle II has been operating successfully in full detector setup since April 2019. The DQM subsystem has performed to expectation: online data quality monitors work and are being optimized for the best usability. The DQM system follows incoming requests and the development of the DAQ system. The lists of monitored values for pixel and strip detectors evolve

according to user requests. Updating of DQM software and reference plots is conservative due to requirements on production system stability but is not frozen. The PXD and SVD detector groups expect that automation of the data acquisition systems and improvements in data quality monitoring will eventually relieve the need for online expert shifts and will allow delegation of the task to central shifters.

Acknowledgments

This project has received funding from the European Union's Horizon 2020 research and innovation programme under the Marie Skłodowska-Curie grant agreements No 644294 and 822070. This work is supported by MEXT, WPI, and JSPS (Japan); ARC (Australia); BMFWF (Austria); MSMT, GAUK 404316 (Czechia); AIDA-2020 (Germany); DAE and DST (India); INFN (Italy); NRF-2016K1A3A7A09005605 and RSRI (Korea); MNiSW (Poland); CNRS/IN2P3 (France), Federal Ministry of Education and Research (BMBF, Germany) and MINECO grant FPA2015-71292-C2-1-P (Spain).

References

- [1] M. French et al., *Design and results from the APV25, a deep sub-micron CMOS front-end chip for the CMS tracker*, Nucl. Instrum. Meth. A **466** (2001) 359-365.
- [2] Edited by: Z. Doležal and S. Uno, *Belle II technical design report*, arXiv:1011.0352v1[physics.ins-det].
- [3] D. Levit, et al.: *FPGA based data read-out system of the Belle II pixel detector*, IEEE Trans. Nucl. Sci. **62** (2015) 1033–1039.
- [4] T. Gessler, et al, *The ONSEN data reduction system for the Belle II pixel detector*, IEEE Trans. Nucl. Sci. **62**(3) (2015) 1149-1154.
- [5] T. Higuchi et al., *Development of a PCI Based Data Acquisition Platform for High Intensity Accelerator Experiments*, arXiv:hep-ex/0305088 (2003).
- [6] A. Moll, *The software framework of the Belle II experiment*, Journal of Physics, **331** (2011) 10.1088/1742-6596/331/3/032024.